

Carbon Restoration for Decarburized Layer in Spring Steel

Y. Prawoto, N. Sato, I. Otani, and M. Ikeda

(Submitted November 20, 2003)

It is well known that decarburization has a bad effect on spring steel strength. This research presents a method to improve the product quality by means of recovering the decarburization layer. Unlike conventional methods, which usually use mechanical means, this method relies on a basic metallurgical principle, the process of diffusion. A carbon-rich layer is coated on the surface of the object. The object is then heat treated at conditions similar to the manufacturing process. To accomplish the objective, an experiment and a finite-element analysis (FEA) simulation were performed. The material chosen was a hypo-eutectoid steel with an excessive decarburization layer. The simulation was performed by digitizing the optical micrograph of decarburized raw materials and meshing the picture to get elements to start the analysis. Simple diffusion theory was then applied to the model. Various time parameters were used to simulate the redistribution of the carbon atoms. Comparable with the simulation, an experiment was also performed. The experiment began by coating a carbon-rich material onto decarburized raw material. The samples were then austenitized and subsequently either annealed or quenched. The state of the carbon restoration was then evaluated. The research concluded that the idea of carbon restoration can be implemented in the manufacturing process.

Keywords carbon restoration, carburizing, decarburization, diffusion

1. Introduction

Today's engineering products are made to be highly optimized, which from a materials viewpoint means that the material has to be almost exactly the same as that of the design. On the other hand, microstructure is always a favorite tool of material scientists as well as the material practitioners. In making a product, any microstructure deviation from the design is unfavorable to the product.

For automotive components, especially coil springs, the same circumstances apply. Coil spring materials are usually hypo-eutectoid alloy steel. Of the abundant selection of the materials, the ones that have chromium (Cr) and vanadium (V) in them are among the popular, economical ones. The combination of these alloying elements allows high ultimate tensile strength, or a high hardness value to be achieved. When a steel of this type is processed by means of proper quenching and tempering, excellent toughness can also be achieved. However, this type of alloy steel is not trouble-free to make. Wires, which are the raw materials for the coil spring, do not always come in the best shape. A medium to severe decarburization layer occasionally accompanies the raw material.

When already decarburized raw materials are processed into a coil spring without eliminating the decarburized layer, the end product of the coils will not be in an optimum metallurgical condition. The decarburized layer will remain in the end prod-

uct, and it is detrimental to the product. A decarburized layer is always softer than the base-material matrix. The effect of shot peening on a material that has a soft surface is not as good as that of a material that has a hard layer on the surface. In some cases, the microstructure even remains ferrite several hundred microns underneath the surface, while the rest of the matrix is tempered martensite, as required by the design. In this situation, the efficiency of the shot peening is greatly reduced. The mechanism of shot peening^[1] can be attributed to the formation of the compressive residual stresses in the surface layer of the material. The compressive residual stress usually decreases the tensile stress in the component by external forces and therefore increases the fatigue life of the material. Also, as compressive stresses are introduced into the surface and subsurface layers by shot peening, fatigue cracks do not easily initiate in (or propagate through) an area under compression; thus, improvements in fatigue strength are achieved. When the decarburized layer is present, this layer, which is softer, will be plastically deformed very easily. This soft layer locally has low ultimate tensile strength as well as low yield strength. As a result, this plastically deformed layer lacks the capability to generate desirable residual stresses that would provide proper strength and durability.

Although the need to eliminate the decarburized layer is obvious, at present no simple metallurgically based elimination method is available. Controlling the heating furnace environment involves a huge investment. Other elimination methods include mechanical-based techniques. In this category, the two most common ways to eliminate the decarburized layer are by peeling and drawing, both of which rely on the mechanical removal of the layer. The former one is similar to machining, in which a small amount of the outer layer is removed. This method produces superior results but is not economical. The second one depends on plastic deformation near the surface. The softer layer near the surface is reduced instead of removed. This method is economical but does not give satisfactory re-

Y. Prawoto, N. Sato, I. Otani, and M. Ikeda, R&D Department, NHK International, 50706 Varsity Court, Wixom, MI 48393. Contact e-mail: yunan.prawoto@nhk-intl.com.

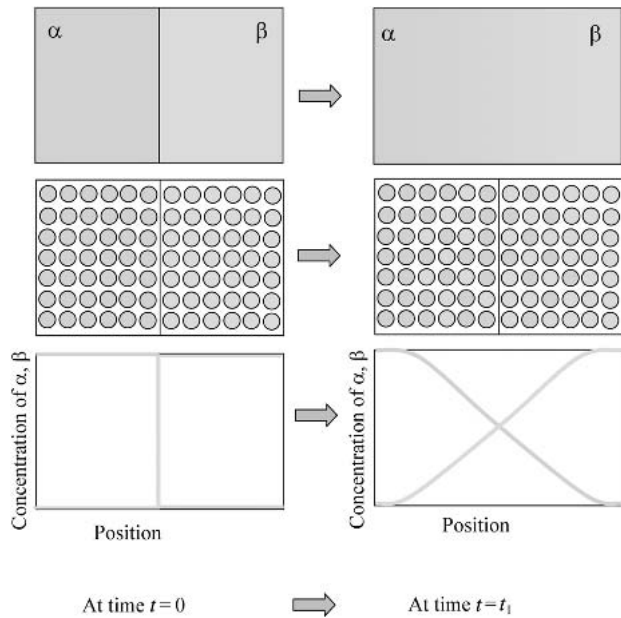


Fig. 1 Illustration of the diffusion couple of α and β after high-temperature heat treatment. The middle pictures show the schematic representation of α and β atoms location within the couple. The lower pictures show the concentration of the α and β atom as a function of position.

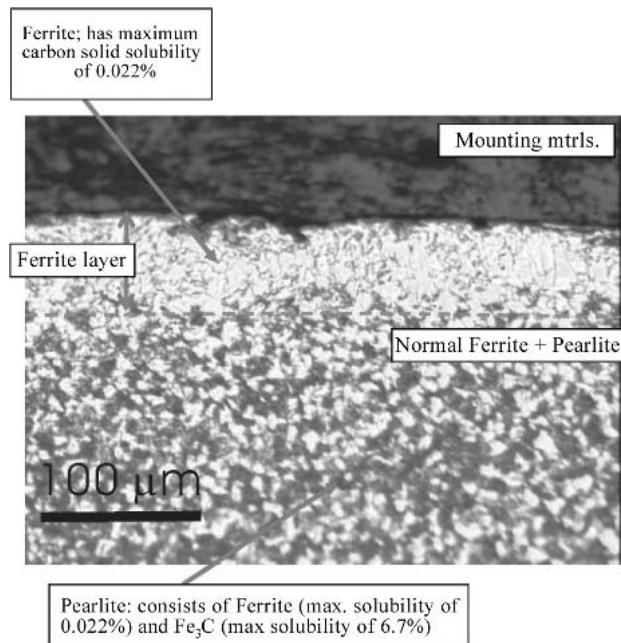


Fig. 2 Typical appearance of raw material with ferrite decarburization layer. The sample was taken from cold-drawn raw materials. When raw material like this is quenched, the majority of the ferrite will remain ferrite, which is detrimental to the product.

sults. With this method, often the decarburized layer is not completely eliminated.

As an alternative method for the elimination of the decarburized layer, a simple metallurgical approach is proposed in



Fig. 3 Samples used for experiment. The upper samples are the non-cold drawn (as rolled), while the lower ones are the cold-drawn materials.



Fig. 4 Appearance of the samples after pretreatment. The pretreatment process includes heating to 400 °C and the addition of the PBC (powder-black compound); carbon-rich material.

Table 1 The Value of the constant used for simulation (C in γ -Fe and in α -Fe)

Symbol	Name	In γ -Fe (bcc)	In α -Fe (fcc)
D_0	Temperature-independent preexponential	$1.0 \times 10^{-5} \text{ m}^2/\text{s}$	$6.2 \times 10^{-7} \text{ m}^2/\text{s}$
Q_d	Activation energy	136 kJ/mol 1.40 eV/atom	80 kJ/mol 0.83 eV/atom
R	Gas constant	8.31 J/mol-K (1.987 cal/mol-K)	

bcc, body-centered cubic; fcc, face-centered cubic

Table 2 Chemical composition of the sample

Composition, wt.%							
C	Si	Mn	Cr	Cu	Ni	Ti	V
0.40	1.80	0.30	1.05	0.25	0.55	0.07	0.17

this research. Similar research has been done in China.^[2] However, due to the language barrier and journal availability, no further details other than the abstract could be obtained.

The research presented here investigated the problem of decarburization and explored the possibility of recovering the

Table 3 Experimental condition

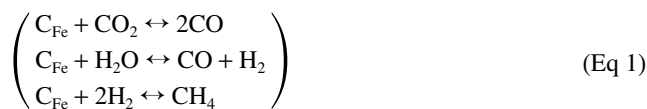
No.	Temperature, °C	Holding time, min	Oil quench/anneal	Remarks
1	n/a	n/a	n/a	As is (no heating)
2	1050	30	Anneal	Simulates the end product
3	1050	30	Oil quench	with no recovery treatment
4	900	10	Anneal	900 °C simulates the Ac ₃ line
5	900	30	Anneal	(minimum austenitizing
6	900	60	Anneal	temperature) for the
7	900	10	Oil quench	corresponding steel.
8	900	30	Oil quench	
9	900	60	Oil quench	
10	1050	10	Anneal	1050 °C is the maximum
11	1050	30	Anneal	temperature that can be
12	1050	60	Anneal	achieved using the furnace
13	1050	10	Oil quench	available in the lab.
14	1050	30	Oil quench	
15	1050	60	Oil quench	

decarburized layer metallurgically. Ultimately, the result of the research gives an embryo to develop a new way to eliminate the decarburized layer based on metallurgy.

2. Background

Decarburization, as the word implies, is a loss of carbon atoms from the surface of the work pieces, thereby producing a surface with lower carbon content than at some other distance beneath the surface. Several standards on decarburization have been developed in industrial societies, e.g., SAE.^[3] In the SAE standard, decarburization is defined as the loss of carbon at the surface of commercial ferrous materials that have been heated for fabrication or when heated to modify mechanical properties. The standard furthermore classifies decarburization into several types.

The phenomenon of decarburization usually takes place at temperatures above about 700 °C, with the following reaction^[4]:



When the reaction goes from the left to right, decarburization occurs.

Decarburization is one of the problems with raw materials available in the market. Depending on the level of the decarburized layer, it can range from a minor to a serious problem and can be detrimental to the end product. The phenomenon of decarburization is known to take place due to long exposure of a steel product to high temperature in air (see reaction in Eq 1). The carbon content is depleted on the outside by means of diffusion. Figure 1 shows how atoms diffuse outside of their original area according to diffusion theory. In the figure, two metal blocks, α and β, are coupled. The metals are then heated to a certain temperature where diffusion can occur. After time $t = t_1$, the α atoms move to the right, while the β atoms move to the left.

For the particular problem of steel, the major alloying element is carbon. The concentration of carbon dictates the prop-

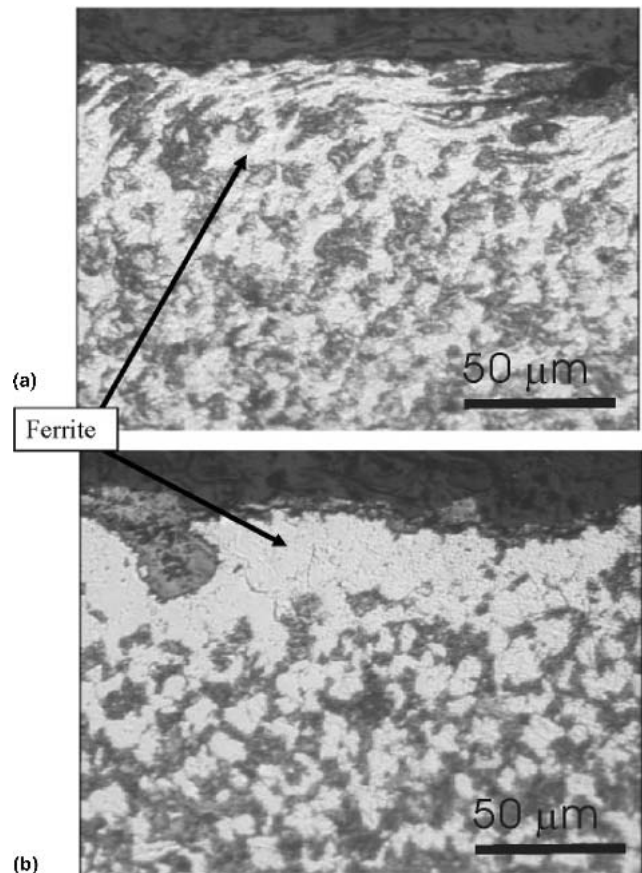


Fig. 5 Microstructure of sample #1 (no treatment). (a) shows the cold-drawn sample and (b) shows the as-rolled sample. Note that even after the cold draw, the ferrite decarburization layer does not completely disappear.

erties of steel. In decarburized steel, because the carbon content is so low, the microstructure remains ferrite even if the material is quenched. It deviates from the desired target microstructure, which is martensite. A typical decarburized layer is shown in Fig. 2, where a layer of ferrite is created on the surface. The reason for this is that the carbon content at the point of interest

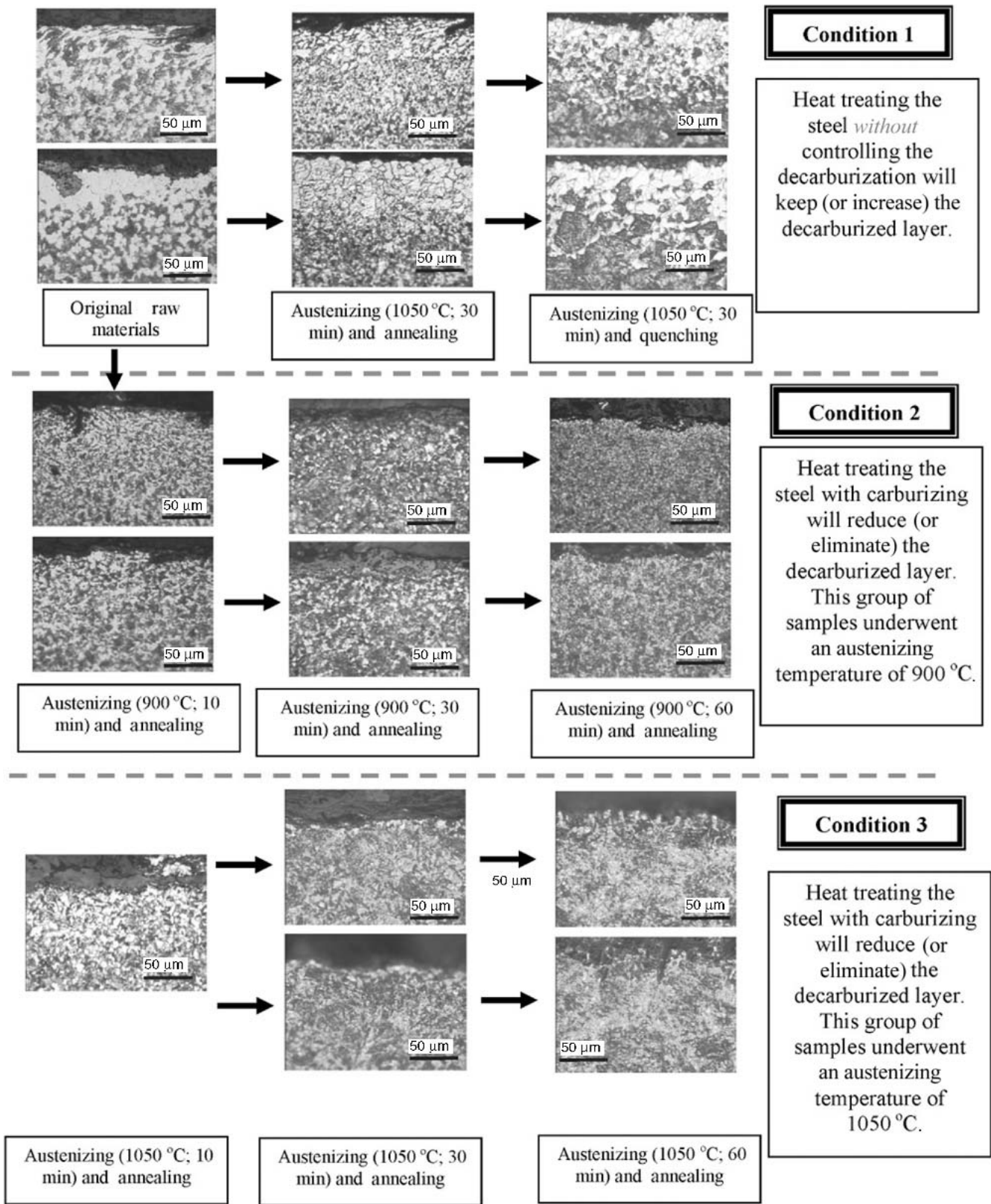


Fig. 5(b) Microstructure of samples subjected to austenizing and annealing. It shows that the carburization can be used to reduce and eliminate the decarburization layer. 30 min of holding time almost completely recovers the decarburization layer.

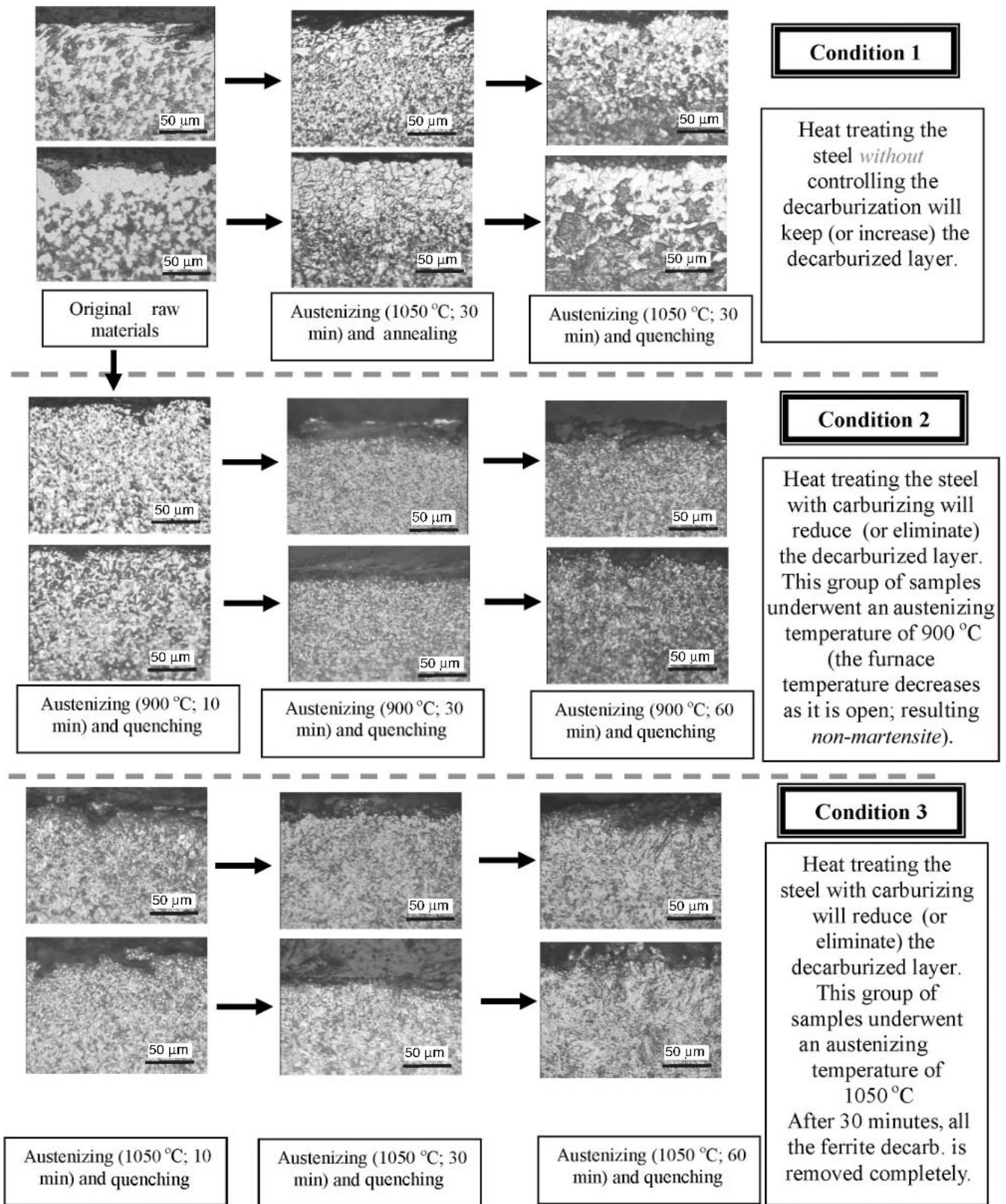


Fig. 5(c) Microstructure of samples subjected to austenitizing and quenching. It shows that the carburization can be used to reduce and eliminate the decarburization layer. 30 min of holding time almost completely recovers the decarburization layer.

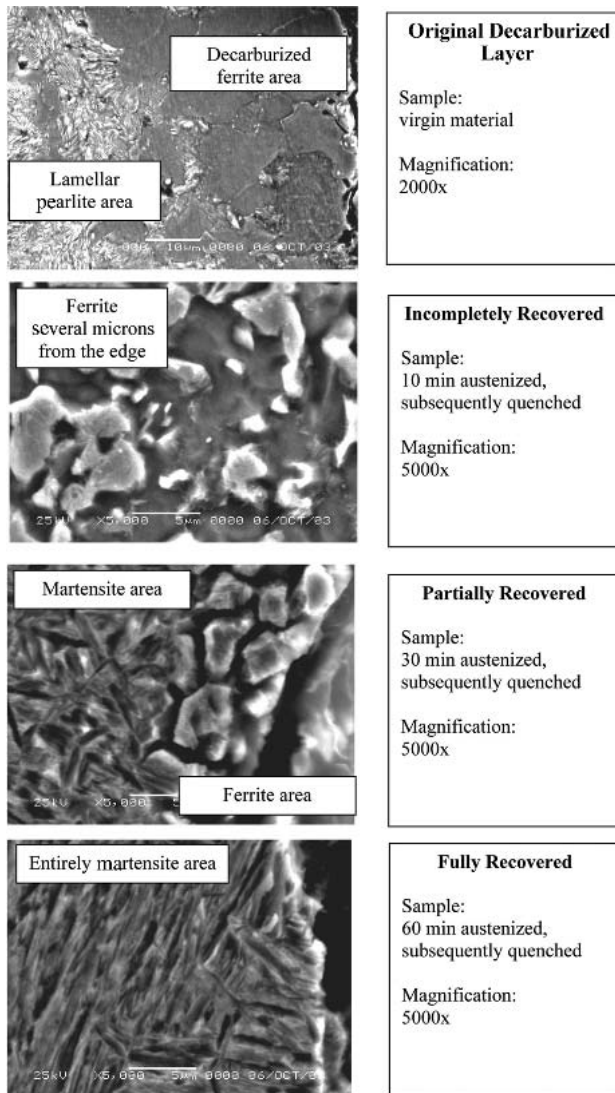


Fig. 5(d) Comparison of the virgin material with processed materials. It shows that the decarburized layer is completely recovered.

is below the solid solubility of the ferrite structure, which is known to be 0.022% in the Fe-C phase diagram. For a material to easily become martensitic after heat treatment, the carbon content at the austenitizing temperature must be above the solid solubility of the ferrite. Only in that case will sufficient carbon atoms be easily entrapped in a preferred position to form martensite.

2.1 Diffusion Mechanisms

From the atomic movement point of view, diffusion is a stepwise migration of atoms from lattice site to lattice site. In fact, the atoms in solid materials are in constant motion, rapidly changing position. For an atom to make such a movement, two conditions must be met. First, there must be an empty adjacent site. Second, the atom must have sufficient energy to break bonds with its neighbor atoms and then cause some lattice distortion during the displacement. At some specific tempera-

ture, some fraction of the atoms are capable of diffusion motion. In general, there are two types of diffusion: vacancy and interstitial.

2.1.1 Vacancy Diffusion. One mechanism involves the interchange of an atom from a normal lattice position to an adjacent vacant lattice site or vacancy. This mechanism is termed vacancy diffusion. This mechanism necessitates the presence of vacancies, and the extent to which vacancy diffusion can occur is a function of the number of these defects that are present. A significant concentration of vacancies may exist in metals at high temperature. Because diffusing atoms and vacancies exchange positions, the diffusion of atoms in one direction corresponds to the motion of vacancies in the opposite direction. Both self-diffusion and interdiffusion occur by this mechanism.

2.1.2 Interstitial Diffusion. The second type of diffusion is interstitial diffusion. It involves atoms that migrate from an interstitial position to a neighboring one that is empty. This mechanism is for impurity atoms in metals. Carbon is considered an impurity atom of iron in steel. The fact that a carbon atom is smaller than the iron atom makes this type of diffusion the preferable mechanism for the both carburization and decarburization. Therefore, from this point on, the discussion is limited to interstitial diffusion.

2.2 Governing Equation of Interstitial Diffusion

The basic governing equation of the diffusion of carbon in the iron matrix is known as Fick's second law.^[5]

$$\frac{\partial C}{\partial t} = \frac{\partial}{\partial x} \left(D \frac{\partial C}{\partial x} \right) \quad (\text{Eq 2})$$

where D is the diffusion coefficient, and C is the concentration. The derivators t and x are time and position, respectively. When the diffusion coefficient is assumed constant and independent of the composition, Eq 2 can be simplified to

$$\frac{\partial C}{\partial t} = D \left(\frac{\partial^2 C}{\partial x^2} \right) \quad (\text{Eq 3})$$

Generally, the diffusion coefficient, D , is known to be temperature dependent, as expressed in:

$$D = D_0 \exp \left(- \frac{Q_d}{RT} \right) \quad (\text{Eq 4})$$

where D_0 is the temperature-independent preexponential, Q_d is the activation energy, R is the gas constant, and T is the absolute temperature. The value of each constant for C in Fe is shown in Table 1.

Equation 3 has a physical meaning when the boundary condition is specified. By making the following three assumptions, the problem is simplified.

- The origin of the system is at the surface ($x = 0$ at the surface, and increases with distance into solid).
- Before diffusion begins, the time t is 0.
- Before diffusion, the concentration of the solid is C_0 .

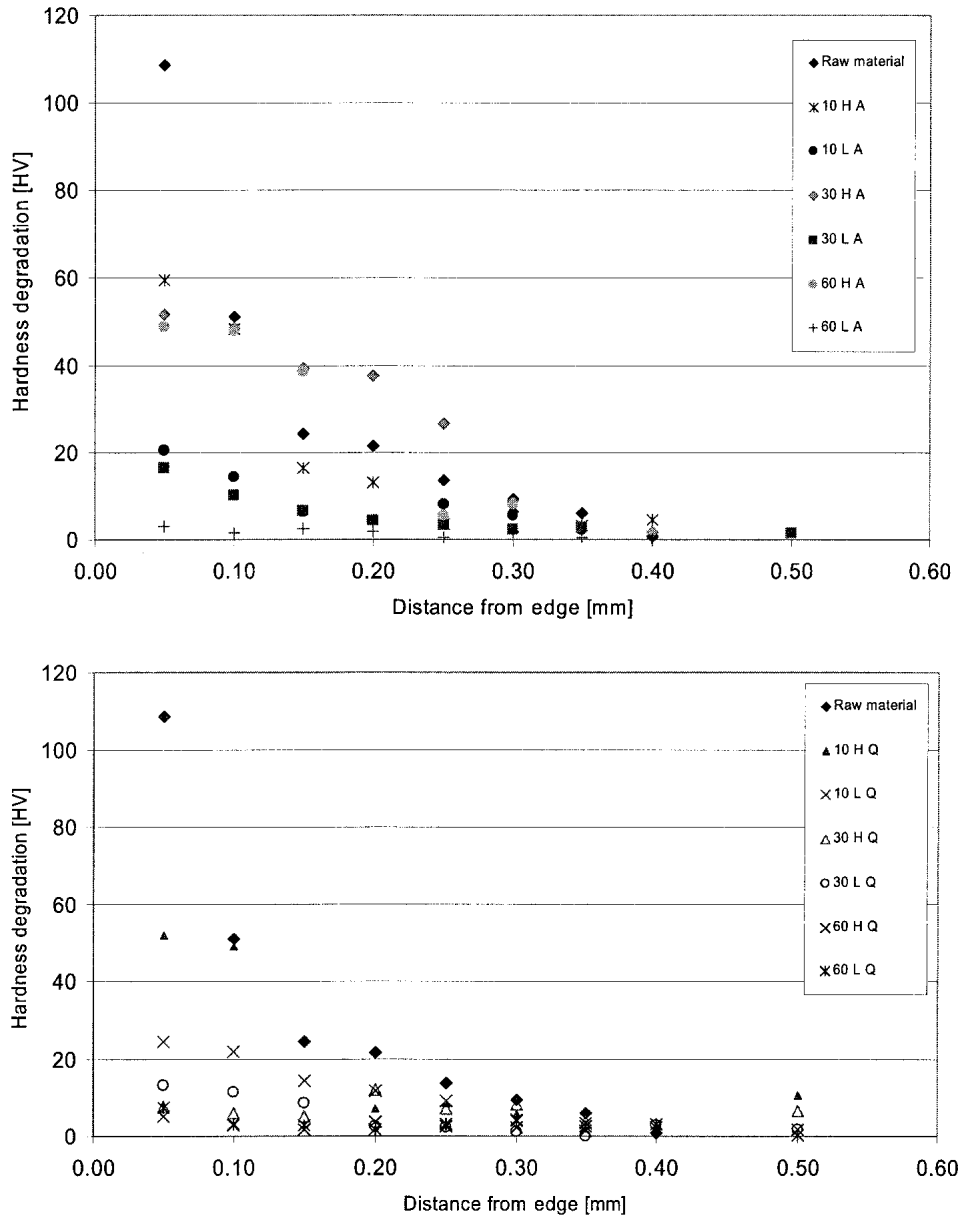


Fig. 6 Hardness degradation near the surface with respect to the center of the sample. The upper graph shows the result of the annealed samples, while the lower one shows that of the quenched samples.

For such conditions, Eq 3 is simplified to:

$$\frac{C_x - C_0}{C_s - C_0} = 1 - \operatorname{erf}\left(\frac{x}{2\sqrt{Dt}}\right) \quad (\text{Eq 5})$$

where C_x is the carbon concentration at the position of x from the metal surface and C_s is the carbon concentration at the surface, which for this case is the carbon-rich coating applied to the surface in this research. The erf is the Gaussian error function, defined by:

$$\operatorname{erf}(z) = \frac{2}{\pi} \int_0^z e^{-y^2} dy \quad (\text{Eq 6})$$

where the z , the term inside the brackets, is equal to $(x/\sqrt{2Dt})$.

Simulation of the diffusion based on Eq 5 was performed. Although when doing so, Fick's second law, Eq 3, was actually used.

3. Experiment Method

The typical composition of the object material, a medium-carbon alloy steel, is shown in Table 2. Based on this material and its corresponding phase diagram, two different temperatures were then chosen, namely at moderately low and high temperatures. The experiments start with selecting the bars that have a ferrite decarburization layer, i.e., above 0.05 mm of Dm-F (metallographic-based ferrite decarburization measure-

ment result). The samples are then cut into pieces. Figure 3 shows the appearance of the samples prior to doing any experiment. All samples are then preheated and coated with a

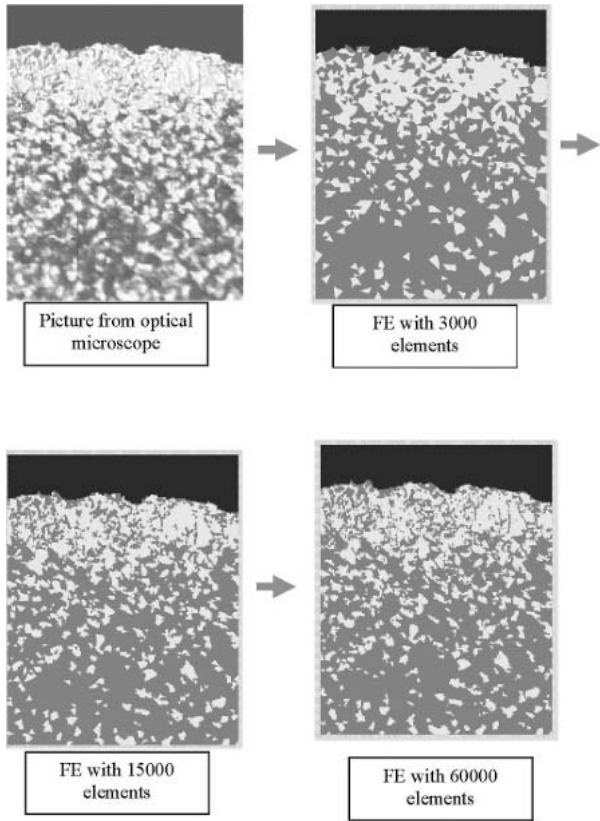


Fig. 7 Finite-element meshing based on the optical microscope, using triangular elements. With approximately 60 000 elements, the model imitates the original optical microscope-based picture.

carbon-rich coating (Rose Mill Corporation, East Hartford, CT). Figure 4 shows the samples after the coating with the PBC (powder-black compound). Prior to doing this, the samples were preheated to 400 °C. By doing so, carbon-rich material can stick to the surface of the samples. Following this step, the samples were then heat treated and quenched using various conditions. Table 3 shows the various heating conditions applied. On all samples, metallographic and microhardness evaluations were performed. Based on these data, the optimum restoration condition was identified.

4. Results

In Fig. 5(a), the original raw materials have quite significant decarburized layers, both the “Dm-F” and “Dm-T.” The term Dm-F refers to the layer where the ferrite-dominated microstructure exists. Similarly, the term Dm-T means “partial decarburization,” which is any measured loss of carbon content less than that of the base material. In this particular sample, the base material has approximately 0.4% C. The ferrite decarburized layer, on the other hand, has less than 0.022%, which means that the raw material has lost a significant amount of carbon.

As the samples were processed, the carbon content near the surface changed. The degree of recovery is seen in Fig. 5(b) and (c), the conditions after annealing and after quenching, respectively. The top pictures in the figures show the heat treatment of the sample having no carbon-rich material coating. Here, one can see that the ferrite layer remains in the material. This situation could eventually lead to the degradation of the material property of the product. Pictures in the middle (condition 2) and at the bottom (condition 3), however, show the appearance of the microstructure with different austenitizing time. One can see that with approximately 60 min of austenitizing time, the ferrite layer is eliminated and becomes mar-

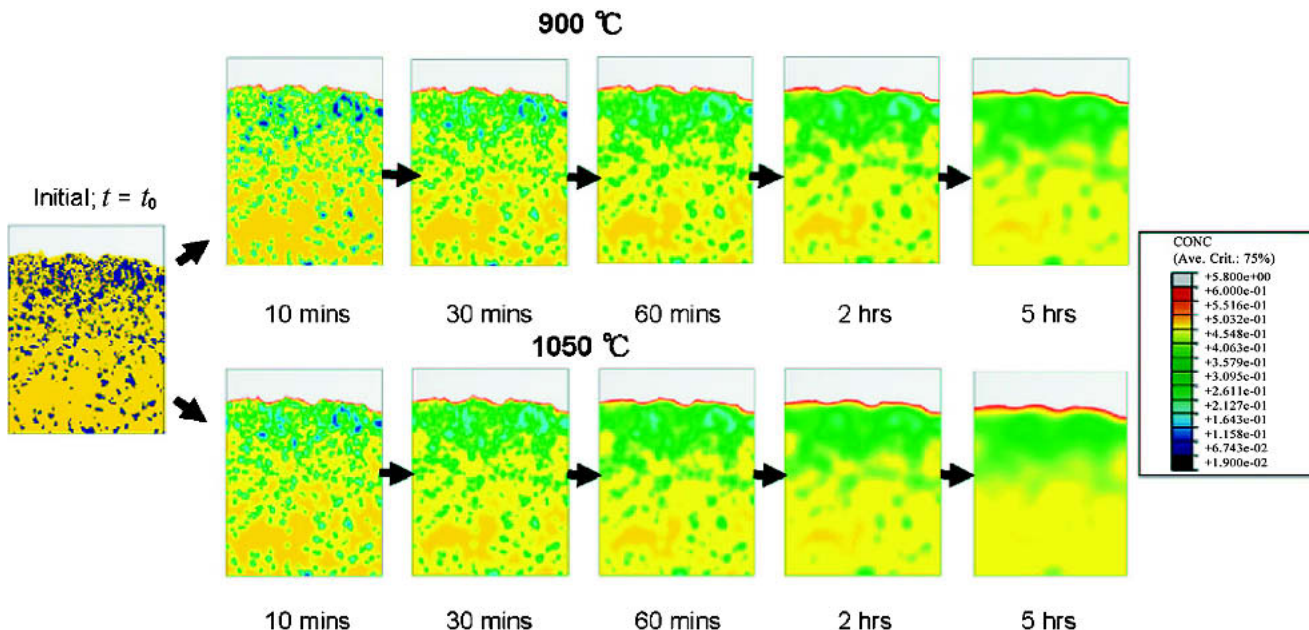


Fig. 8 The result of the FEA shows that the carbon diffuses into the layer and eliminates the decarburized layer.

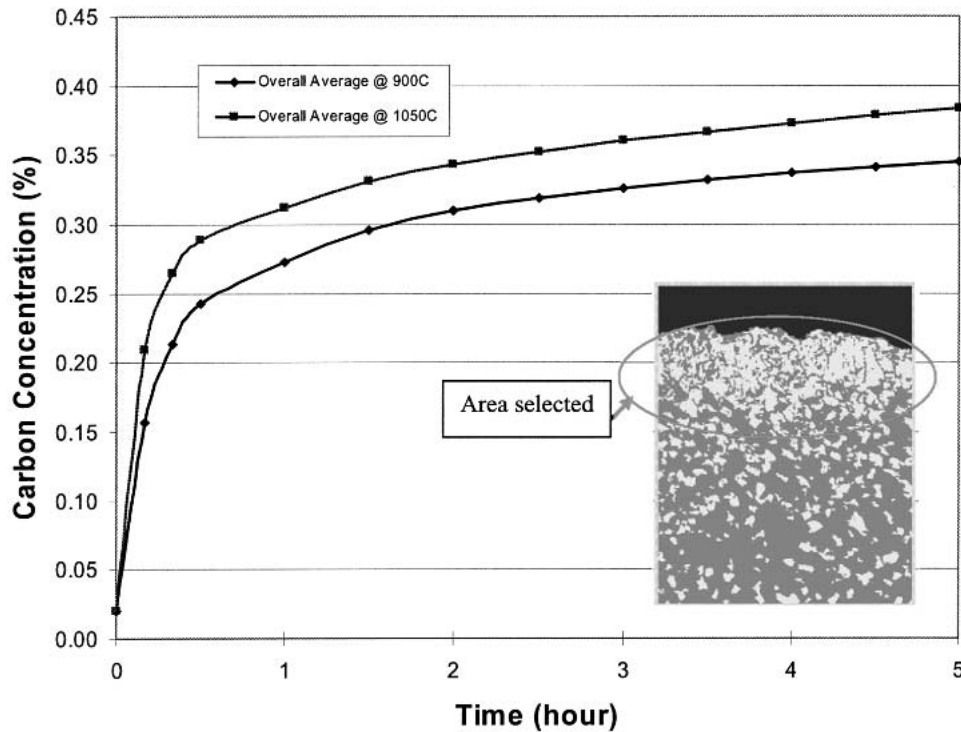


Fig. 9 Analysis result of the carbon concentration as the austenitizing continues at a particular point. The point is shown in the inserted picture. The overall graph, however, is taken from the overall element originally possessing a ferrite structure.

tensite, or pearlite. This term means that the carbon content is recovered. The detailed SEM picture of the microstructure near the surface is shown in Fig. 5(d). The bottom picture in the figure shows that after 60 min of austenitizing, the entire microstructure becomes martensite.

Figure 6 shows the result of the microhardness evaluation. One can see that the hardness loss caused by the decarburization is reduced significantly by the process. The longer the austenitizing time is, the less discrepancy between the hardness near the edge and the core. This fact also emphasizes that carbon restoration is an effective way to eliminate the decarburized layer.

5. Analysis

5.1 Analysis Method

The analysis began with converting the image taken by an optical microscope into a digital image. A finite-element (FE) model was then created, using PPM2OOF.^[6] Figure 7 shows the model with triangular elements. In the figure, the digitized picture of the microstructure as well as its corresponding FE models are shown. With approximately 60 000 elements, one can see that the model is much better than that of 3000 or 15,000 elements. Further meshing could have produced an even better resolution. However, in this research, the meshing was terminated after only 60,000 elements, the last picture shown in Fig. 7. The reason for choosing this number of elements is mainly for calculation efficiency.

The nodes and elements generated at PPM2OOF are then

exported to a commercial FE software. Here, ABAQUS^[7] was used for the purpose of the analysis. The carbon-rich material has 5.8% C; while that of the ferrite and pearlite, respectively, are 0.02% and 0.49%. The DC2D3 (a three-node linear mass diffusion element) was used. The time increment was 0.1667 h between 0 and 0.5 h, 0.5 h between 0.5 and 5 h.

5.2 Analysis Result

The analysis result is shown in Fig. 8. In the figure, one can see that the carbon diffused into the steel material. With a 1050 °C austenitizing temperature, the carbon content reached a value of approximately 0.4%, which is the typical carbon content of the base material. The same condition also applies after 60 min with a lower temperature. To a great extent, the simulation performed here is in agreement with experimental results.

Figure 9 shows the carbon content increment of one representative element located approximately 20 μm underneath the surface. One can see that the carbon concentration increases as the austenitizing continues. Again this result is also in agreement with the experiment. At high temperatures, the diffusion speed is higher, which leads to a faster increase of carbon content. In the same figure, one can also find that the first 30 min of austenitizing are the most efficient at eliminating the ferrite decarburization layer.

6. Conclusions

An overview of the decarburization phenomenon and its recovery using basic diffusion concepts has been presented.

Experiment and analysis to support the concept were performed. Both experiment and analysis proved that carbon restoration within the decarburized layer via diffusion can be accomplished. For the particular steel used in this research, austenitizing the sample for 30 min recovered the ferrite decarburization. The optimum condition for recovering the decarburization layer is heating at 1050 °C for 30 min. Extending the time to 60-120 min completely recovered the decarburized layer, as suggested by analysis results. The use of this concept, in principle, can be extended to any type of the decarburized layer with an adjustment of the carbon concentration of the material to infuse the carbon. Austenitizing time and temperature are the two parameters that can be adjusted to accomplish this procedure.

References

1. S. Tekeli: "Enhancement of Fatigue Strength of SAE 9245 Steel by Shot Peening," *Mater. Lett.*, 2002, 57, p. 604.
2. J. Hao, "Carbon Restoration Process for High and Medium Carbon Steel After Decarburization," *Chinese Appl. Exper. J. JA*, 10(25), 1994, (in Chinese).
3. SAE International, *2003 SAE Handbook - Vol. 1*, Society of Automotive Engineers, Warrendale, PA, 2003.
4. G. Parrish, *Carburizing: Microstructures and Properties*, ASM International, Materials Park, OH, 1999.
5. W.F. Smith, *Foundations of Materials Science and Engineering*, Irwin/McGraw-Hill, New York, 1993.
6. W.C. Carter, S.A. Langer, and E.R. Fueller, *OOF Manual*, NISTIR 6256, 1998.
7. HKS, Inc., *Abacus/Standard Users Manual*, Version 6.3, Pawtucket, RI, 2002.